Published online September 26, 2005

Nucleic Acids Research, 2005, Vol. 33, No. 17 ***5521–5532***
doi:10.1093/nar/gki872

Regulation of multiple insulin-like growth factor binding protein genes by 1α,25-dihydroxyvitamin D_3

Merja Matilainen, Marjo Malinen, Katri Saavalainen and Carsten Carlberg*

Department of Biochemistry, University of Kuopio, P.O. box 1627 IN-70211 Kuopio, Finland

Received June 8, 2005; Revised and Accepted September 12, 2005

ABSTRACT

Recently, insulin-like growth factor binding proteins (IGFBPs) have been found to be primary mediators of the anti-proliferative actions of the nuclear hormone 1α,25-dihydroxyvitamin D_3 [1α,25$(OH)_2D_3$], but dependent on cellular context IGFBPs can also have a mitogenic effect. In this study, we performed expression profiling of all six human *IGFBP* genes in prostate and bone cancer cells and demonstrated that *IGFBP1*, *3* and *5* are primary 1α,25$(OH)_2D_3$ target genes. *In silico* screening of the 174 kb of genomic sequence surrounding all six *IGFBP* genes identified 15 candidate vitamin D response elements (VDREs) close to or in *IGFBP1*, *2*, *3* and *5* but not in the *IGFBP4* and *6* genes. The putative VDREs were evaluated *in vitro* by gelshift assays and in living cells by reporter gene and chromatin immuno-precipitation (ChIP) assays. Of these 10 VDREs appear to be functional. ChIP assays demonstrated for each of these an individual, stimulation time-dependent association profile not only with the vitamin D receptor, but also with first heterodimeric partner the retinoid X receptor, other regulatory complex components and phosphorylated RNA polymerase II. Some of the VDREs are located distantly from the transcription start sites of *IGFBP1*, *3* and *5*, but all 10 VDREs seem to contribute to the regulation of the genes by 1α,25$(OH)_2D_3$. In conclusion, *IGFBP1*, *3* and *5* are primary 1α,25$(OH)_2D_3$ target genes that in intact cells are each under the control of multiple VDREs.

INTRODUCTION

The biologically most active vitamin D metabolite, 1α,25-dihydroxyvitamin D_3 [1α,25$(OH)_2D_3$], is essential for mineral homeostasis and skeletal integrity (1). However, it also has important roles in the control of the growth and differentiation in normal tissues and malignant cells derived from prostate, breast and bone (2). 1α,25$(OH)_2D_3$ mainly acts as a nuclear hormone and mediates its genomic effects via the nuclear receptor vitamin D receptor (VDR) (3). The anti-proliferative effects of 1α,25$(OH)_2D_3$ include induction of a G_1/G_0 cell cycle arrest and stimulation of apoptosis, which are mediated by the up-regulation of tumor suppressors, such as the cyclin-dependent kinase inhibitory proteins p21 and p27 (4), and the down-regulation of oncogene products including Bcl-2 (5) and Myc (6). Mitogens, such as the insulin-like growth factors (IGFs), have also been reported to be down-regulated by 1α,25$(OH)_2D_3$ (7). In addition, also the up-regulation of factors which control the actions of mitogens, such as IGF binding proteins (IGFBPs), have important anti-cancer effects (8). Unfortunately, many of the genes involved in these processes, such as the *p27* and *bcl-2*, are secondary 1α,25$(OH)_2D_3$ targets (9). However, the *IGFBP3* gene was shown to be a primary VDR target (10) and is therefore of special interest for understanding the mechanisms of the cell-regulatory actions of 1α,25$(OH)_2D_3$. IGFBP3 belongs to the six-member IGFBP family that bind IGFs with high affinity and specificity (11). IGFBPs also mediate IGF-independent actions, including inhibition of cell growth and induction of apoptosis (12). Since gene families often encode products, which have overlapping functions, we wondered if this was also true at the level of responsiveness to a particular ligand. Therefore, we focused in this study on the regulation of the *IGFBP* gene family by 1α,25$(OH)_2D_3$.

An essential prerequisite for the direct modulation of transcription by 1α,25$(OH)_2D_3$ is the location of at least one activated VDR protein close to the transcription start site (TSS) of the respective primary 1α,25$(OH)_2D_3$ target gene. This is achieved through the specific binding of VDR to a vitamin D response element (VDRE) (13). In detail, the DNA-binding domain of the VDR contacts the major groove of a double-stranded hexameric DNA sequence with the optimal RGKTCA (R = A or G, K = G or T) core binding sequence. VDR binds as a dimer to DNA and in most cases the nuclear receptor retinoid X receptor (RXR) is its heterodimeric partner (13). Simple VDREs are therefore formed by two hexameric core binding motifs in a direct repeat (DR) or everted repeat

*To whom correspondence should be addressed. Tel: +358 17 163062; Fax: +358 17 2811510; Email: carlberg@messi.uku.fi

(ER) orientation. The optimal spacing for DR-type VDREs was found to be 3 and 4 nt (DR3 and DR4) (14,15) and that of ER-type VDREs 7 to 9 nt (ER7, ER8 and ER9), respectively (16,17). Although individual VDREs have been shown to be able to induce transactivation on their own, the presence of multiple VDREs in any given regulatory region will allow a more flexible and complex regulation of the respective gene. Recently, we have shown that the primary 1α,25(OH)$_2$D$_3$ target genes *CYP24* (18) and *cyclin C* (19) each contain four functional VDREs within the first 10 kb of their promoter region. In the promoter of the human *IGFBP3* gene only one DR3-type VDRE so far has been reported, which is located ~3.2 kb upstream of the TSS (10). However, this does not exclude the presence of additional VDREs.

Binding of VDR to a VDRE is a central step in 1α,25(OH)$_2$D$_3$ signaling. In the absence of ligand, corepressor proteins, such as SMRT, NCoR and Alien (20), link DNA-bound VDR to enzymes with histone deacetylase activity that cause chromatin condensation (21). This provides VDR with intrinsic repressive properties comparable with both retinoic acid and thyroid hormone receptors (20). Ligand binding to the VDR causes a conformational change within its ligand-binding domain that results in the replacement of corepressors by coactivator proteins of the p160-family, such as SRC-1, TIF2 and RAC3 (22). These coactivator proteins link ligand-activated VDR to enzymes displaying histone acetyltransferase activity, that cause chromatin relaxation and thereby reversing the action of unliganded VDR (23). In a subsequent step, ligand-activated VDR changes rapidly from interacting with p160-coactivators to those of the mediator complex, such as TRAP220/DRIP205 (24). The mediator complex acts as a bridge from activated VDR to the basal transcriptional machinery (25). In this way ligand-activated VDR executes two tasks, the modification of chromatin and the regulation of transcription.

In this study, we performed expression profiling of all six human *IGFBP* gene family members in prostate and bone cancer cells and demonstrated that the genes *IGFBP1*, *3* and *5* are primary 1α,25(OH)$_2$D$_3$ targets. *In silico* screening of all *IGFBP* genes identified 15 candidate VDREs close to *IGFBP1*, *2*, *3* and *5*, but none within *IGFBP4* and *6*. Of these 10 VDREs seem to be functional and chromatin immunoprecipitation (ChIP) assays demonstrated that for each of them an individual, ligand-stimulation time-dependent association profile with VDR, RXR, SMRT, SRC-1, TRAP220 and phosphorylated RNA polymerase II (P-Pol II). Some of the VDREs are located rather distantly from the TSS of the *IGFBP1*, *3* and *5*, but all 10 functional VDREs appear to contribute to their regulation by 1α,25(OH)$_2$D$_3$.

MATERIALS AND METHODS

Cell culture

The human prostate cancer cell line PC-3 and the human osteosarcoma cell line SaOS-2 were cultured in DMEM containing 10% fetal bovine serum (FBS), while for the human breast cancer cell line MCF-7, α-MEM supplemented with 5% FBS was used. Both media also contained 2 mM L-glutamine, 0.1 mg/ml streptomycin and 100 U/ml penicillin and the cells were kept in a humidified 95% air/5% CO_2 incubator. FBS was stripped of lipophilic compounds, such as endogenous 1α,25(OH)$_2$D$_3$, by stirring it with 5% activated charcoal (Sigma–Aldrich, St Louis, MO) for 3 h at room temperature. Charcoal was then removed by centrifugation and sterile filtration. Prior to mRNA or chromatin extraction, cells were grown overnight in phenol red-free DMEM supplemented with 5% charcoal-stripped FBS to reach a density of 50–60% confluency. Cells were treated then with solvent (ethanol, 0.1% final concentration) or 10 nM 1α,25(OH)$_2$D$_3$ (kindly provided by Dr Lise Binderup, LEO Pharma, Ballerup, Denmark) for up to 24 h for RNA extractions and for up to 4 h for chromatin preparations.

RNA extraction and real-time quantitative PCR

Total RNA was extracted using the Mini RNA Isolation II kit (Zymo Research, HiSS Diagnostics, Freiburg, Germany) and cDNA synthesis was performed for 1 h at 37°C using 1 µg of total RNA as a template, 100 pmol oligodT_{18} primer and 40 U RT (Fermentas, Vilnius, Lithuania). Real-time quantitative PCR was performed in an IQ-cycler (BioRad, Hercules, CA) using the dye SybrGreen I (Molecular Probes, Leiden, The Netherlands). For each reaction, 1 U Hot Start *Taq* polymerase (Fermentas) and 3 mM $MgCl_2$ were used and the PCR cycling conditions were: 45 cycles of 30 s at 95°C, 30 s at 62°C and 40 s at 72°C. The gene-specific primer pairs (and product sizes) were as follows: *IGFBP1* gene, forward 5′-CACAGGAGACATCAGGAGAAG-3′ and reverse 5′-GAGCTTTGGAAGAGCAGAAATG-3′ (507 bp); *IGFBP2* gene, forward 5′-GATGACCACTCAGAAGGAG-3′ and reverse 5′-CTGCTGCTCATTGTAGAAGAG-3′ (257 bp); *IGFBP3* gene, forward 5′-AAGTTGACTACGAGTCTCAG-3′ and reverse 5′-AATCAGTTCACCACAAACAGA-3′ (439 bp); *IGFBP4* gene, forward 5′-CACGAGGACCTCTACATCATC-3′ and reverse 5′-CAGGACTCAGACTCAGACTC-3′ (297 bp); *IGFBP5* gene, forward 5′-GTCAAGATCGAGAGAGACTC-3′ and reverse 5′-GAAGGTTTGCACTGCTTTCTC-3′ (370 bp); *IGFBP6* gene, forward 5′-GTGTCCAAGACACTGAGATG-3′ and reverse 5′-CAACACCAACACTCTTTCCAAC-3′ (404 bp); *p27* gene, forward 5′-GAGAAGCACTGCAGAGACAT-3′ and reverse 5′-AAGAATCGTCGGTTGCAGGT-3′ (242 bp) and *acidic riboprotein P0* (*ARP0*, also known as *36B4*) control gene, forward 5′-AGATGCAGCAGATCCGCAT-3′ and reverse 5′-GTGGTGATACCTAAAGCCTG-3′ (318 bp). The control gene *ARP0* was checked against a second control gene *RPL13A* and neither gene was found to be affected by any of the treatments at the time points used (data not shown). PCR product quality was monitored using post-PCR melt curve analysis. Fold inductions were calculated using the formula $2^{-(\Delta\Delta Ct)}$, where $\Delta\Delta Ct$ is the $\Delta Ct_{(1\alpha,25(OH)2D3)} - \Delta Ct_{(Ethanol)}$, ΔCt is $Ct_{(IGFBPn \text{ or } p27)} - Ct_{(ARP0)}$ and Ct is the cycle at which the threshold is crossed.

DNA constructs

Full-length cDNAs for human VDR (15) and human RXRα (26) were subcloned into the T_7/SV40 promoter-driven pSG5 expression vector (Stratagene, LaJolla, CA). The same constructs were used for both T_7 RNA polymerase-driven *in vitro* transcription/translation of the respective cDNAs and for viral promoter-driven overexpression in mammalian cells. Each

Table 1. Sequence and position of putative REs within the human IGFBP1, 2, 3 and 5 genes

RE	Type	Gene	Position	Strand	Gene area	Sequence
rANF	DR3	*rat* ANF	−907	+	promoter	agAGGTCAtgaAGGACA
RE1	DR3	IGFBP1	−4533	−	promoter	tcGGTTCTggaAGATCA
RE2	ER7	IGFBP1	−3111	+	promoter	TGACCCctgccagGGGGCA
RE3	DR3	IGFBP1/3	+5327	+	intergenic	ctGGGGCAggcGGGGCA
RE4	ER7	IGFBP1/3	+15359	+	intergenic	TGAACTtggagatAGGTCA
RE5	ER7	IGFBP1/3	+18886	+	intergenic	TGAACTccacagaAGTTCA
RE6	DR3	IGFBP3	−387	−	promoter	cgGGGTCAaggAGATCG
RE7	DR3	IGFBP3	−396	−	promoter	taAGGGCGgcgGGGTCA
RE8	DR3	IGFBP3	−3347	+	promoter	gaGGTTCAccgGGTGCA
RE9	DR3	IGFBP2	+17676	+	1st intron	aaAGGTCAgagGGGGCA
RE10	DR4	IGFBP2	+24655	−	1st intron	agGGTTCAttgaGGGGCA
RE11	DR3	IGFBP2/5	+35665	−	intergenic	ctGGTTCAttcAGATCA
RE12	DR3	IGFBP2/5	+37171	+	intergenic	gtGGGTTAtatGGGTCG
RE13	ER9	IGFBP5	+7775	+	1st intron	TGACCCatcacagccAGTTCA
RE13+	ER11	IGFBP5	+7775	+	1st intron	TGACCCacatcacagccAGTTCA
RE14	DR4	IGFBP5	−4679	+	promoter	atAGGGCAgagcAGGGCA
RE15	ER8	IGFBP5	−7384	+	promoter	TGAACCgaaagctgGGTTCA

The known DR3-type VDRE of the rat ANF gene (28) serves as a comparison. Capital letters indicate hexameric core binding sites. The position of the RE is given relative to the TSS of the indicated gene.

two copies of the VDREs derived from the rat atrial natriuretic factor (ANF) (27) and the 15 candidate response elements (REs) of the *IGFBP* genes (for sequence see Table 1) were fused with the *thymidine kinase* promoter driving the firefly *luciferase* reporter gene. All constructs were verified by sequencing.

Transfection and luciferase reporter gene assays

MCF-7, PC-3 and SaOS-2 cells were seeded into 6-well plates (10^5 cells/ml) and grown overnight in phenol red-free DMEM supplemented with 5% charcoal-stripped FBS. Plasmid DNA containing liposomes were formed by incubating a reporter plasmid and the expression vector for human VDR (each 1 µg) with 10 µg *N*-[1-(2,3-Dioleoyloxy)propyl]-*N*,*N*,*N*-trimethylammonium methylsulfate (DOTAP, Roth, Karlsruhe, Germany) for 15 min at room temperature in a total volume of 100 µl. After dilution with 900 µl phenol red-free DMEM, the liposomes were added to the cells. Phenol red-free DMEM supplemented with 500 µl 15% charcoal-stripped FBS was added 4 h after transfection. At this time, 100 nM 1α, $25(OH)_2D_3$ or solvent were also added. The cells were lysed 16 h after onset of stimulation using reporter gene lysis buffer (Roche Diagnostics, Mannheim, Germany). The constant light signal luciferase reporter gene assay was performed as recommended by the supplier (Canberra-Packard, Groningen, The Netherlands). Luciferase activities were normalized with respect to protein concentration and induction factors were calculated as the ratio of luciferase activity of ligand-stimulated cells to that of solvent controls.

Gelshift assay

In vitro translated VDR and RXR proteins were generated by coupled *in vitro* transcription/translation using their respective pSG5-based full-length cDNA expression constructs and rabbit reticulocyte lysate as recommended by the supplier (Promega, Madison, WI). Protein batches were quantified by test translation in the presence of [^{35}S]methionine. The specific concentration of the receptor proteins was adjusted to ∼4 ng/µl (10 ng corresponds to ∼0.2 pmol) after taking the individual number of methionine residues per protein into account. Gelshift assays were performed with 10 ng of the appropriate *in vitro* translated proteins. The proteins were incubated for 15 min in a total volume of 20 µl binding buffer (150 mM KCl, 1 mM DTT, 0.2 µg/µl poly(dI-C), 5% glycerol and 10 mM HEPES, pH 7.9). Constant amounts (1 ng) of [^{32}P]-labeled double-stranded oligonucleotides (50 000 c.p.m.) containing one copy of the respective REs (Table 1) were then added and incubation was continued for 20 min at room temperature. Protein–DNA complexes were resolved by electrophoresis through 8% non-denaturing polyacrylamide gels (mono- to bisacrylamide ratio 19:1) in 0.5x TBE (45 mM Tris–HCl, 45 mM boric acid and 1 mM EDTA, pH 8.3) for 105 min at 200 V and quantified on a FLA-3000 reader (Fuji, Tokyo, Japan) using ScienceLab99 software (Fuji).

ChIP assays

Nuclear proteins were crosslinked to genomic DNA by adding formaldehyde for 15 min directly to the medium to a final concentration of 1%. Crosslinking was stopped by adding glycine to a final concentration of 0.125 M and incubating for 5 min at room temperature on a rocking platform. The medium was removed and the cells were washed twice with ice-cold phosphate-buffered saline (PBS) (140 mM NaCl, 2.7 mM KCl, 1.5 mM KH_2PO_4 and 8.1 mM $Na_2HPO_4 \bullet 2H_2O$). The cells were collected by scraping in ice-cold PBS supplemented with a protease inhibitor cocktail (Roche Diagnostics). After centrifugation the cell pellets were resuspended in lysis buffer (1% SDS, 10 mM EDTA, protease inhibitors and 50 mM Tris–HCl, pH 8.1) and the lysates were sonicated to result in DNA fragments of 300–1000 bp in length. Cellular debris was removed by centrifugation and the lysates were diluted 1:10 in ChIP dilution buffer (0.01% SDS, 1.1% Triton X-100, 1.2 mM EDTA, 16.7 mM NaCl, protease inhibitors and 16.7 mM Tris–HCl, pH 8.1). Non-specific background was removed by incubating the chromatin resuspension with a salmon sperm DNA/protein A agarose slurry (Upstate Biotechnology,

Lake Placid, NY) for 30 min at 4°C with agitation. The samples were centrifuged and the recovered chromatin solutions were incubated with 5 µl of indicated antibodies overnight at 4°C with rotation. The antibodies against VDR (sc-1008), RXRα (sc-553), SMRT (sc-1610), SRC-1 (sc-7216), TRAP220 (sc-5334), P-Pol II (sc-13583), IgG (sc-2027) and p53 (sc-6243) were obtained from Santa Cruz Biotechnologies (Heidelberg, Germany). The immuno-complexes were collected with 60 µl of protein A agarose slurry (Upstate Biotechnology) for 2 h at 4°C with rotation. The beads were pelleted by centrifugation for 1 min at 4°C at 100× *g* and washed sequentially for 5 min by rotation with 1 ml of the following buffers: low salt wash buffer (0.1% SDS, 1% Triton X-100, 2 mM EDTA, 150 mM NaCl and 20 mM Tris–HCl, pH 8.1), high salt wash buffer (0.1% SDS, 1% Triton X-100, 2 mM EDTA, 500 mM NaCl and 20 mM Tris–HCl, pH 8.1) and LiCl wash buffer (0.25 mM LiCl, 1% Nonidet P-40, 1% sodium deoxycholate, 1 mM EDTA and 10 mM Tris–HCl, pH 8.1). Finally, the beads were washed twice with 1 ml TE buffer (1 mM EDTA and 10 mM Tris–HCl, pH 8.0). The immuno-complexes were then eluted by adding 250 µl elution buffer (1% SDS and 100 mM $NaHCO_3$) and incubation for 15 min at room temperature with rotation. After centrifugation, the supernatant was collected and the elution was repeated. The supernatants were combined and the cross-linking was reversed by adding NaCl to final concentration of 200 mM and incubating overnight at 65°C. The remaining proteins were digested by adding proteinase K (final concentration 40 µg/ml) and incubation for 1 h at 45°C. Genomic DNA fragments were recovered using the Qiaex II Gel Extraction Kit (Qiagen, Hilden, Germany).

PCR of chromatin templates

For each of the 14 candidate RE-containing genomic regions and the TSS of the genes *IGFBP1*, *2*, *3* and *5* primer pairs were designed (Table 2), optimized and controlled by running PCRs with 25 ng genomic DNA (input) as a template. When running immuno-precipitated DNA (output) as a template, following PCR profile was used: preincubation for 5 min at 94°C, 40 cycles of 30 s at 95°C, 30 s at 60°C and 30 s at 72°C and one final incubation for 10 min at 72°C. The PCR products were separated by electrophoresis through 2.0% agarose. Dye SybrGreen (1 µl) (1:2500 dilution) was added to each sample before loading. Gel images were scanned on a Fuji FLA3000 reader using ScienceLab99 software.

Table 2. Genomic PCR primers

Region (gene)	Location	Primer sequences (5′–3′)
1 *(IGFBP1)*	−4371 to	CTCTACATCTTTGAGGGTGGG
	−4156	GACGTGGGAGAATCGTTTGAG
2 *(IGFBP1)*	−3246 to	CTGCACTTCCCAGAGCTGAG
	−3062	GTTACAGCCGATGATGTGAC
3 *(IGFBP1/3)*	+5077 to	CTGTGGTGATGTTGCCACCTG
	+5415	GAGGATGGGGACTAATGGAGAG
4 *(IGFBP1/3)*	+15255 to	GAGAACTAAATGGAAATGCTGGAG
	+15576	CTGGAATAAATCCCACTGATCATG
5 *(IGFBP1/3)*	+18796 to	CTTACTAGGCAGCGTTCTCATG
	+19008	CTGTCTACCAGCGACAACCAAC
6/7 *(IGFBP3)*	−280 to	GTCACCTTGTCGTCTACAAG
	−483	CACGAGGTACACACGAATGC
8 *(IGFBP3)*	−3286 to	CTGGAGTGACTCACCAGAGTC
	−3465	CTTGCCTGCCTCTCTCAGCTG
9 *(IGFBP2)*	+17599 to	GAATGTGTCCTGAGTGCCAG
	+17734	GTCCTGAGACTTTGTGGGTG
10 *(IGFBP2)*	+18965 to	GTTACTCCATGTTGGTCAGACTG
	+19136	GAGATTCACTCACGAGTCAGAAC
11 *(IGFBP2/5)*	+35559 to	CATGAACTGCAACTGTGATGTC
	+35740	CAATAAGCCACCAGGTGCTAG
12 *(IGFBP2/5)*	+37095 to	GAGACAGGAGTGGAGTAGTC
	+37295	CACACTGCCTGGAGCAGGTG
13 *(IGFBP5)*	+7887 to	CTGTCTGTTCCTCATACATTC
	+7635	CTCCCTTGTTTGGTCCCTAG
14 *(IGFBP5)*	−4572 to	GAGCCAGCTGTGACGCAGAG
	−4740	GAACATGCCAGATCCCATGATC
15 *(IGFBP5)*	−7275 to	GATGGCTCTGTACTCAAGGAG
	−7535	CTCAGAGGATAAGTCCTGAGTC
IGFBP1 TSS	−100 to	GAACACTCAGCTCCTAGCGTG
	+153	CTGACATCTCCAGGCGCGAG
IGFBP3 TSS	−129 to	GAGCAGCACCAGCAGAGTC
	+92	CAGGGATGGGGCGACAGTAC
IGFBP2 TSS	−62 to	GAAGGGAGTGGTCTCCAAAAG
	+117	CACTCTCGGCAGCATGCTG
IGFBP5 TSS	−32 to	GTTCTACGCGAAGTCCGGAG
	+92	CTCCTTGGCATCCTTGCCTG

Sequence and location of the primer pairs used to detect genomic regions containing putative VDREs or TSS within the IGFBP1 and 3 and IGFBP2 and 5 gene pairs. The location is indicated in relation to the closest TSS.

RESULTS

Basal expression of *IGFBP* gene family members in prostate and bone cancer

The basal mRNA expression levels of all six members of the *IGFBP* gene family were monitored by real-time quantitative PCR in relation to the control gene *ARP0* in PC-3 human prostate cancer (Figure 1A) and SaOS-2 human osteosarcoma cells (Figure 1B). In both cell lines the genes *IGFBP4* and *6* showed the highest expression, but in SaOS-2 cells these maximal levels were ∼10-fold lower than in PC-3 cells. In PC-3 cells the mRNA amount of *IGFBP1* and *3* was ∼15-fold lower, that of *IGFBP-2* >300-fold lower and that of *IGFBP5* even 12 000-fold lower than that of *IGFBP4* and *6* (Figure 1A). In contrast, in SaOS-2 cells the differences in the expression of the *IGFBP* gene family members showed less pronouced differences, since the mRNA levels of *IGFBP3* and *5* were only ∼3-fold lower and that of *IGFBP1* and *2* only 30-fold lower than that of *IGFBP4* and *6* (Figure 1B).

IGFBP1, *3* and *5* are primary 1α,25(OH)$_2$D$_3$ target genes

PC-3 and SaOS-2 cells were treated for 24 h with 10 nM 1α,25(OH)$_2$D$_3$ in the absence or presence of the protein translation inhibitor cycloheximide in order to differentiate between primary and secondary effects of the VDR ligand. The relative fold induction of the mRNA amounts of the six *IGFBP* genes and of the known secondary 1α,25(OH)$_2$D$_3$ target gene *p27* (9) were determinded by real-time quantitative PCR (Figure 1C and D). In PC-3 cells the genes *IGFBP1*, *3* and *5* were found to be 2- to 4-fold induced by 1α,25(OH)$_2$D$_3$ and this induction was not significantly modulated by the presence of cycloheximide (Figure 1C). The three other *IGFBP* gene family members and the *p27* gene showed in this cell line no response to the natural VDR ligand. In SaOS-2 cells the genes *IGFBP1*, *3* and *5* were also 2- to

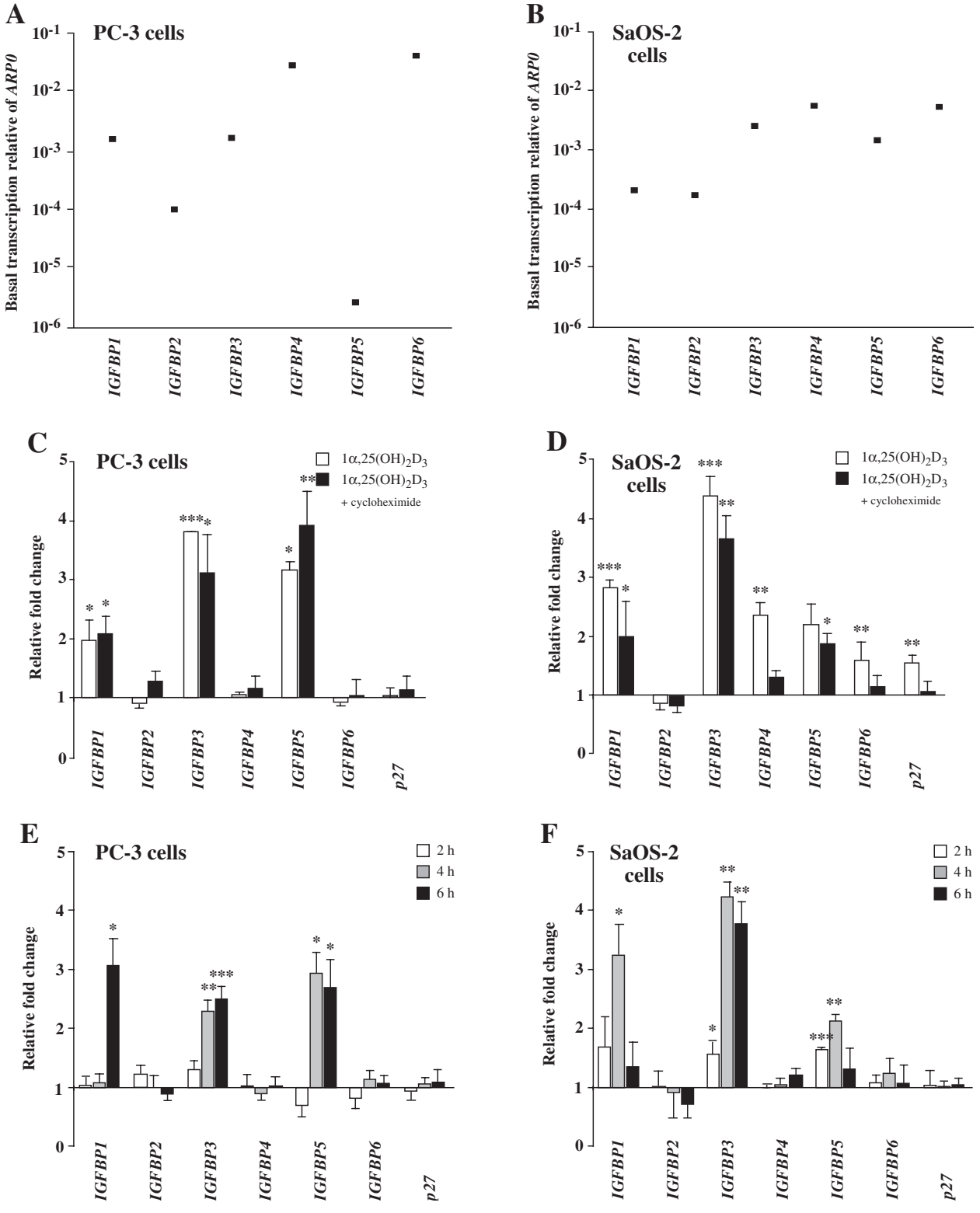

Figure 1. Expression profiling of the human *IGFBP* gene family in prostate and bone cancer cells. Real-time quantitative PCR was used to determine the ratio of the basal mRNA expression of the six *IGFBP* genes relative to the control gene *ARP0* in PC-3 (**A**) and SaOS-2 cells (**B**). A logarithmic scale is employed on the *Y*-axis to better present the data. In the same cell lines, the induction of mRNA levels of the six *IGFBP* genes and of the known secondary $1\alpha,25(OH)_2D_3$ target gene *p27* after a 24 h treatment with 10 nM $1\alpha,25(OH)_2D_3$ was determined in the absence and presense of 10 μM cycloheximde (**C** and **D**). The early time course (2 to 6 h) of the mRNA expression of all seven genes in response to 10 nM $1\alpha,25(OH)_2D_3$ was also measured in PC-3 (**E**) and SaOS-2 (**F**) cells. Data points (A and B) and columns (C–F) indicate the means of at least three independent cell treatments and the bars represent standard deviations. The standard deviations in (A and B) are too small to be visible in relation to the data points. Two-tailed Student's *t*-tests were performed to determine the significance of the mRNA induction by $1\alpha,25(OH)_2D_3$ in reference to solvent controls (*$P < 0.05$, **$P < 0.01$, ***$P < 0.001$).

4-fold inducible by 1α,25(OH)$_2$D$_3$ without being significantly affected by cycloheximide (Figure 1D). Interestingly, in this cell line even the genes *IGFBP4*, *IGFBP6* and *p27* responded 1.5- to 2.2-fold to 1α,25(OH)$_2$D$_3$ treatment, but this induction disappeared in the presence of cycloheximide. This observation indicates that the *IGFBP4* and *6* gene are only secondary 1α,25(OH)$_2$D$_3$ targets as is known for the *p27* gene. The *IGFBP2* gene did not respond at all to ligand treatment.

Next, we performed in both cell lines a time course analysis of the early mRNA expression of all six *IGFBP* genes and the *p27* gene in response to 1α,25(OH)$_2$D$_3$ over 2, 4 and 6 h (Figure 1E and F). In confirmation of the results obtained in Figure 1C and D, only the *IGFBP1*, *3* and *5* gene, but neither the genes *IGFBP2*, *4* and *6* nor the *p27* gene responded within this time frame to the natural VDR ligand. After 4 and 6 h of ligand treatment the response of the *IGFBP3* gene showed a stable 2.5- and 4-fold induction in PC-3 and SaOS-2 cells, respectively. In contrast, the expression of the genes *IGFBP1* and *5* demonstrated a more cell-specific profile (compare Figure 1E and F). In PC-3 cells *IGFBP1* mRNA was induced 3-fold after 6 h of stimulation with 1α,25(OH)$_2$D$_3$, while in SaOS-2 cells it showed a comparable peak already after 4 h. Moreover, in PC-3 cells *IGFBP5* mRNA expression was after 4 and 6 h constantly 3-fold increased, while in SaOS-2 cells it displayed a smaller peak of only 2-fold induction after 4 h stimulation with ligand. Taken together, in both cell lines the genes *IGFBP1*, *3* and *5* but not *IGFBP2*, *4* and *6* are primary 1α,25(OH)$_2$D$_3$ target genes.

In silico screening for putative VDREs

Based on a list of >15 known natural VDREs (28) we obtained the consensus hexameric core sequence RGDKYR (R = G or A, D = A,G or T, K = G or T, Y = C or T) and used it to screen *in silico* the gene area (defined as 10 kb upstream of the TSS until the end of the last exon) of each of the six human *IGFBP* genes for putative VDREs. Since the genes *IGFBP1* and *3* as well as *IGFBP2* and *5* are found adjacent to each other in the genome (Figure 2), we also screened the intergenic area between these two gene pairs. For the specific search for VDREs we considered only hexameric core sequence pairs in DR3, DR4, ER6, ER7, ER8 or ER9 orientation. Moreover, we kept only RE candidates formed of hexamers with maximal two deviations from the optimal RGKTCA core binding sequence in our list and excluded putative VDREs being located in Alu repetitive sequence (representing ~12% of the 174 kb genomic sequence screened in total). These restrictions finally resulted in 15 putative VDREs, of which two (REs 1 and 2) were located in the area of the *IGFBP1* gene, three (REs 3, 4 and 5) between the genes *IGFBP1* and *3*, three (REs 6, 7 and 8) in the *IGFBP3* gene, two (REs 9 and 10) in the *IGFBP2* gene, two (REs 11 and 12) between the genes *IGFBP2* and *5* and three (REs 13, 14 and 15) in the *IGFBP5* gene (Figure 2). In contrast, no REs were found in the genes *IGFBP4* and *6*.

The majority (eight) of the REs are of DR3-type. There were also two DR4-type, three ER7-type, one ER8-type and one ER9-type REs (Table 1). The DR3-type RE8 in the promoter of the *IGFBP3* gene has already been described as a functional VDRE (10), whereas the 14 remaining putative VDREs are novel. Interestingly, REs 6 and 7 form a composite RE of three hexameric binding motifs. Moreover, all REs were screened in the database dbSNP (www.ncbi.nlm.nih.gov/SNP) for known small nucleotide polymorphisms (SNPs) and for RE13 a 2 nt insertion variation was found (RE13+ in Table 1), which was included in the following RE evaluation. In summary, *in silico* screening resulted in 15 putative VDREs in the genes *IGFBP1*, *2*, *3* and *5*, but none in the genes *IGFBP4* and *6*. This result is mostly in agreement with the observation that the genes *IGFBP1*, *3* and *5* but not *IGFBP2*, *4* and *6* are primary 1α,25(OH)$_2$D$_3$ targets.

Functionality of putative VDREs within the *IGFBP* genes

The functionality of the 15 putative VDREs identified *in silico*, the SNP variation of RE13 (RE13+) and the reference DR3-type VDRE of the rat *ANF* gene (27) was assessed by reporter gene assays in transiently transfected MCF-7 breast cancer cells (Figure 3A), PC-3 cells (Figure 3B) and SaOS-2 cells (Figure 3C). MCF-7 cells represent an established 1α,25(OH)$_2$D$_3$ responding cell line (19) and were chosen as reference to other studies. Two copies of each of the 15 putative VDREs, RE13+ and the rat *ANF* VDRE were fused with the *thymidine kinase* promoter driving the firefly *luciferase* reporter gene. The response to 1α,25(OH)$_2$D$_3$ of the three different cell lines transfected with these constructs was monitored after 16 h. As expected, MCF-7 cells showed the highest inducibilty by 1α,25(OH)$_2$D$_3$: compared with the 16.9-fold inducibility of the reference VDRE, REs 8, 2 and 13 were

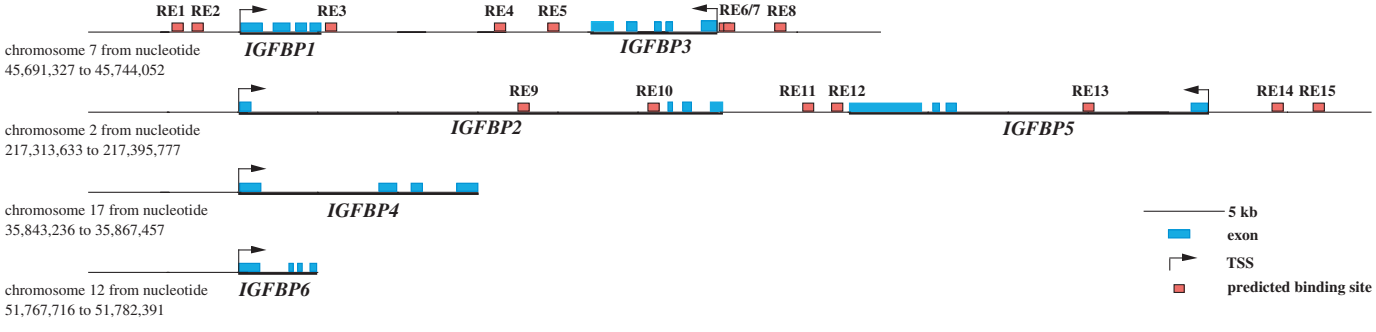

Figure 2. Overview on the genomic organization and location of the six human *IGFBP* family members. Human genomic DNA (174 kb) (thin black line) from four different chromosomes comprising all six human *IGFBP* genes were screened *in silico* for putative VDREs. Fifteen candidate REs (red boxes) were identified in the genes *IGFBP1*, *2*, *3* and *5* but none in *IGFBP4* and *6*. The sequences of the REs are indicated in Table 1.

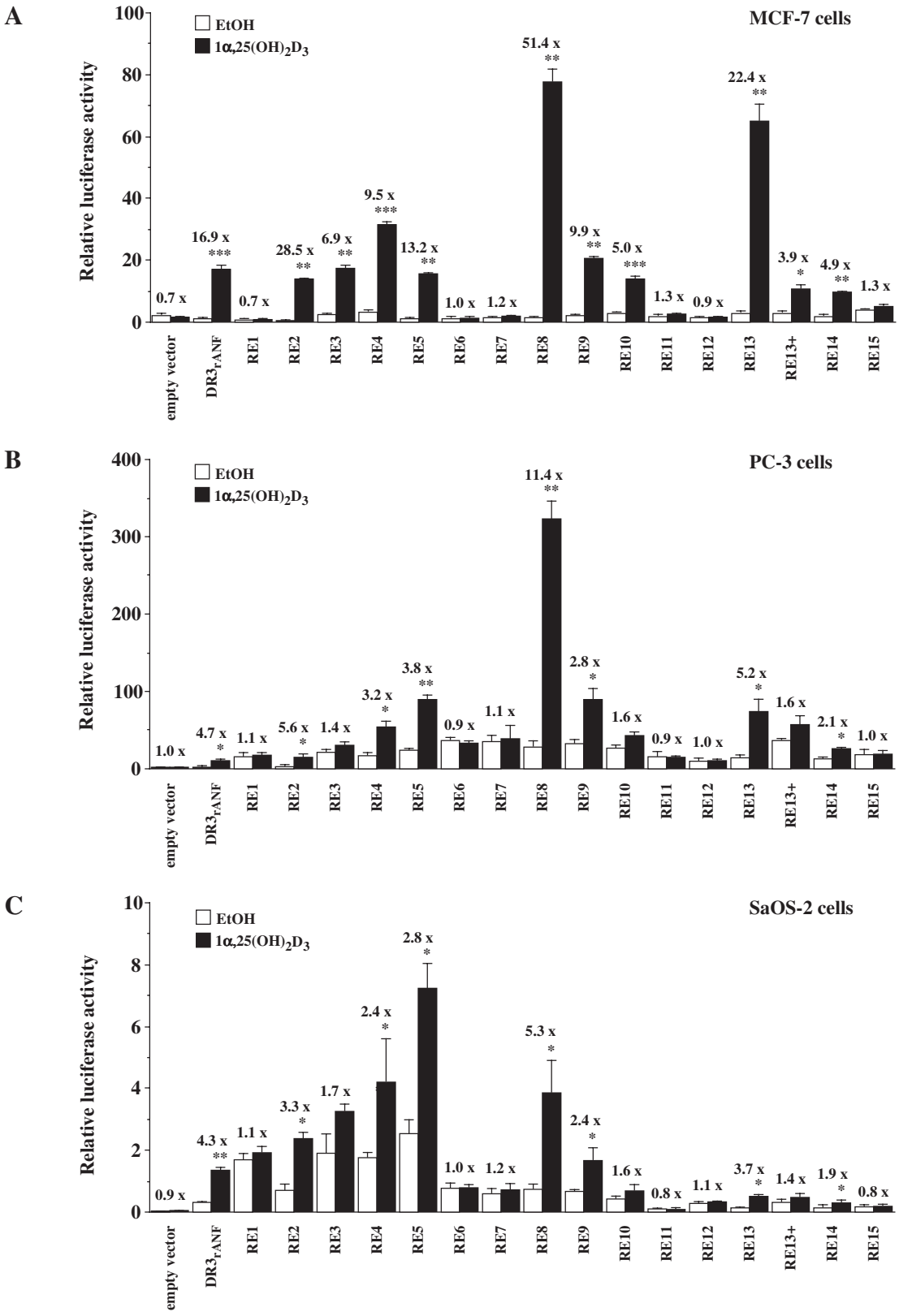

Figure 3. Functionality of putative VDREs derived from human *IGFBP* genes. Reporter gene assays were performed with extracts from MCF-7 cells (**A**), PC-3 cells (**B**) and SaOS-2 cells (**C**) that were transiently transfected with *luciferase* reporter constructs each containing two copies of one of the 15 candidate VDREs and the SNP variation of RE13 (RE13+) or of the rat *ANF* DR3-type VDRE and an expression vector for human VDR. Cells were treated for 16 h with either solvent or 100 nM $1\alpha,25(OH)_2D_3$. Relative luciferase activity is shown and fold inductions are indicated above the columns. Columns represent means of at least three experiments and bars indicate SDs. Two-tailed Student's *t*-tests were performed to determine the significance of reporter gene induction by $1\alpha,25(OH)_2D_3$ in reference to solvent controls (*$P < 0.05$, **$P < 0.01$, ***$P < 0.001$).

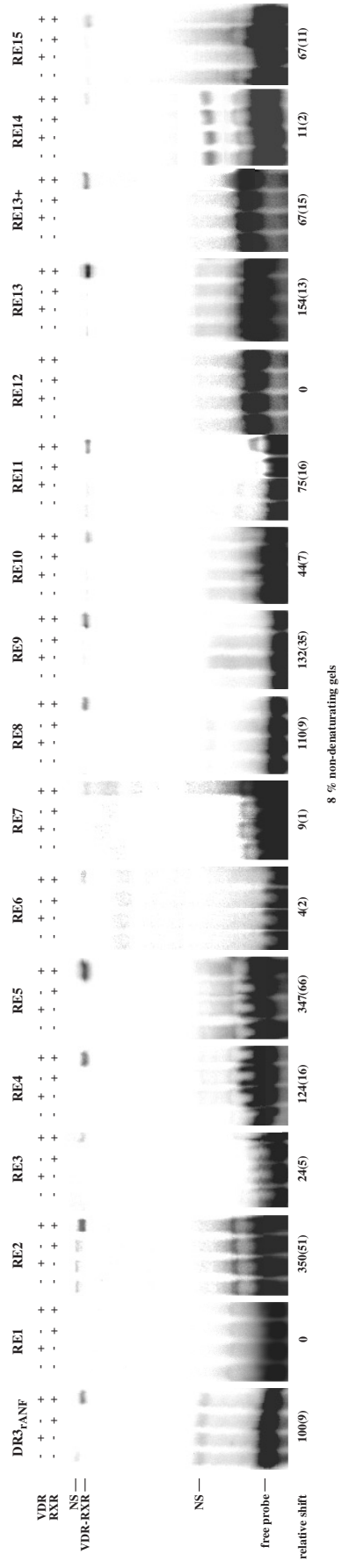

even more potent with a 51.4-, 28.5- and 22.4-fold induction of reporter gene activity (Figure 3A). The 13.2-, 9.9-, 9.5-, 6.9-, 5.0- and 4.9-fold induction mediated by two copies of the REs 5, 9, 4, 3, 10 and 14, respectively, indicate that they are able to function as VDREs. In contrast, the SNP variation RE13+ lost significantly its $1\alpha,25(OH)_2D_3$ responsiveness and therefore represents a less efficient VDRE. Moreover, neither the absolute reporter gene activity nor the inducibility of REs 1, 6, 7, 11, 12 and 15 was sufficient for a functional VDRE.

The inducibility of PC-3 (Figure 3B) and SaOS-2 cells (Figure 3C) were in average 5- and 10-fold lower than that of MCF-7 cells, but concerning relative inducibility all three cell lines provided similar results. RE8 was in all cells more inducible than the reference VDRE, RE13 showed a comparable inducibility than the reference VDRE and also REs 2, 4, 5, 9 and 14 demonstrated a statistically significant inducibility by $1\alpha,25(OH)_2D_3$ in all tested cell lines. However, owing to cell-specific variations in the basal activity of the reporter gene constructs carrying the different REs, the absolute activities of the REs do not match perfectly between the three different cell lines.

In vitro characterization of putative VDREs within the *IGFBP* genes

To assess the relative VDR–RXR heterodimer binding, gelshift assays were performed using *in vitro* translated VDR and RXR proteins either alone or in combination and the 15 putative VDREs of the *IGFBP* genes (Figure 4). The conditions were identical to our earlier DR3-type VDRE comparative study (28) and the DR3-type VDRE of the rat *ANF* gene was chosen again as reference. The ER7-type REs 2 and 5 bound 3.5-fold more effectively VDR–RXR heterodimers than the reference DR3-type VDRE and also the ER9-type RE13 and the ER7-type RE4 were 1.5- and 1.2-fold stronger, respectively. Moreover, the DR3-type REs 9, 8 and 11 showed with 132, 110 and 75% of the binding of the reference RE good affinity for VDR–RXR heterodimers. Finally, the ER8-type RE15 (67% heterodimer binding capacity) and the DR4-type RE10 (44%) can be considered as VDREs as well. Interestingly, the ER11-type SNP variation of RE13 (RE13+) still showed 67% binding capacity of the reference VDRE (which equals 44% of RE13). In contrast, the binding of VDR–RXR heterodimers to the REs 1, 3, 6, 7, 12 and 14 was too low in our stringent assay conditions to consider them as efficient VDREs. Taken together, according to standardized *in vitro* criteria developed in our previous studies (28), 7 (REs 4, 8, 9, 10, 11, 13 and 15) of the 15 candidate REs show 0.5- to 1.5-fold of DNA-binding capacity of the reference VDRE and can be considered as good VDREs. In addition, two REs (REs 2 and 5) even demonstrated a 3.5-fold higher

Figure 4. *In vitro* analysis of the putative VDREs derived from the human *IGFBP* gene areas. Gelshift experiments were performed with *in vitro* translated human VDR and human RXR alone or in combination and in the presence of different [^{32}P]-labeled REs representing the 15 candidate VDREs and the SNP variation of RE13 (RE13+) of the human *IGFBP* genes and the rat *ANF* DR3-type reference VDRE. Protein–DNA complexes were resolved from free probe through non-denaturing 8% polyacrylamide gels. Representative gels are shown. The relative amount of VDR–RXR heterodimer complex formation was quantified on a FLA-3000 reader in relation to the reference VDRE. Numbers below the gels indicate the means of at least three independent gel shift experiments and their SDs are given in brackets. NS indicates non-specific complexes.

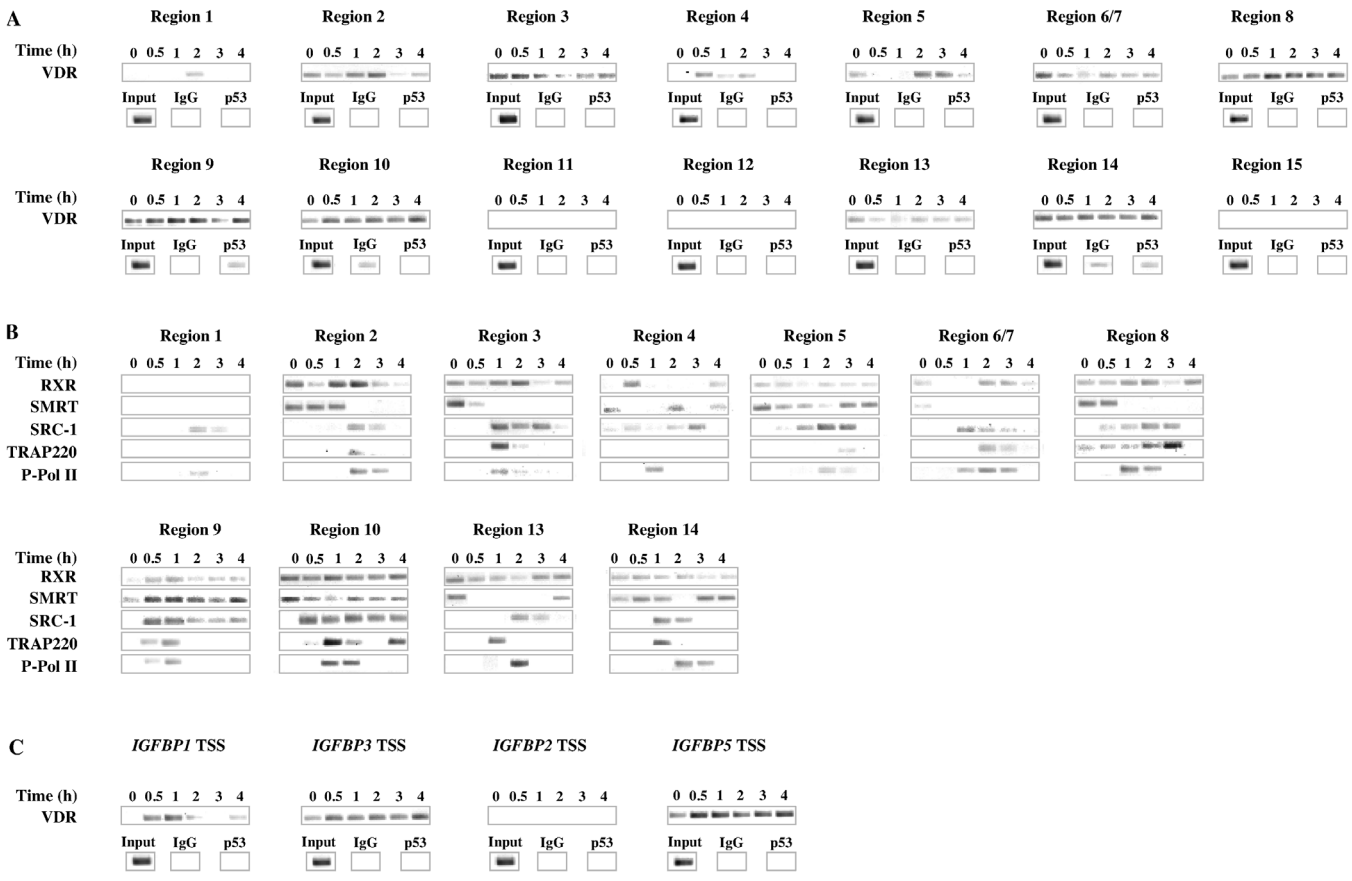

Figure 5. Association of RE-containing genomic regions and proximal promoters of *IFGBP* genes with VDR and other nuclear proteins. Chromatin was extracted from PC-3 cells that had been treated for indicated time periods with 10 nM $1\alpha,25(OH)_2D_3$. ChIP experiments were performed with anti-VDR, anti-RXR, anti-SMRT, anti-SRC-1, anti-TRAP220 or anti-P-Pol II antibodies. Anti-IgG and anti-p53 antibodies were used as non-specific controls. These display some background signal for the regions 9, 10 and 14. The association of VDR and its partner proteins was monitored on the 14 RE-containing genomic regions (**A** and **B**) of the genes *IGFBP1*, *2*, *3* and *5* and their proximal promoters (**C**). Representative agarose gels are shown.

DNA-binding affinity than the reference VDRE and should be considered as high affinity VDREs.

Overall there is good correlation between the reporter gene assay results (Figure 3) and the *in vitro* analysis (Figure 4). REs 2 and 13 are confirmed as very good VDREs and REs 1, 6, 7 and 12 showed no response in either of the two assays. The response of RE8 in the functional assay was higher and that of RE5 lower than expected, but both REs appeared to be very effective VDREs. Finally, REs 4 and 9 were also confirmed as VDREs. In summary, a number of VDREs (REs 2, 4, 5, 8, 9 and 13) were shown to respond effectively to $1\alpha,25(OH)_2D_3$ and its receptor in both evaluation series.

Functionality of putative VDREs in chromatin context of living cells

We next examined whether VDR was located to the genomic regions containing these REs in living cells. Chromatin was extracted from PC-3 cells which had been grown overnight in the presence of 5% charcoal-treated FBS, stimulated for 0, 0.5, 1, 2, 3 and 4 h with 10 nM $1\alpha,25(OH)_2D_3$ and then crosslinked for 15 min in the presence of formaldehyde. ChIP assays were performed using an antibody against VDR. The genomic DNA fragments that were recovered from reverse-crosslinked chromatin served as templates for PCRs with primers specific for the regions containing the 15 putative VDREs (Table 2). Since REs 6 and 7 are in the same region, they cannot be detected separately and therefore represented together. Representative agarose gels of the PCR products from all treatment times are shown (Figure 5A). The input lane serves as a reference for comparable detection sensitivity for the 14 genomic regions within the *IGFBP1* and *3* and *IGFBP2* and *5* gene tandems (Figure 2) and ChIP assays using IgG or anti-p53 antibody served as controls. Interestingly, with the exception of regions 11, 12 and 15, on the remaining 11 genomic regions VDR binding could be detected (Figure 5A). On some of the latter regions, such as regions 2, 3, 6/7, 8, 9, 10, 13 and 14, VDR binding was found in the absence of ligand. Moreover, $1\alpha,25(OH)_2D_3$ treatment did not significantly affect the binding of its receptor to these genomic regions, but on some regions (2, 8, 9 and 10) the tendency of a maximal binding after 2 h could be observed. Only on regions 1, 4 and 5 a significant $1\alpha,25(OH)_2D_3$-dependent modulation of the VDR association could be detected.

For a deeper analysis of the 11 VDR-associated regions of the *IGFBP1/3* and *2/5* gene cluster, further ChIP assays were performed with antibodies against RXR, the corepressor SMRT, the coactivator SRC-1, the mediator protein TRAP220 and P-Pol II (Figure 5B). With the exception of region 1, on the remaining 10 genomic regions RXR

association was found. This RXR binding was not significantly modulated by 1α,25(OH)$_2$D$_3$ treatment in most cases. In the latter aspect, the binding of SMRT to the 10 VDR- and RXR-positive genomic regions provided a clearer picture. In the absence of ligand SMRT binding was detected on all 10 regions containing a putative VDRE with the exception of regions 9 and 10. This SMRT binding was diminished after 30–120 min of 1α,25(OH)$_2$D$_3$ treatment. Interestingly, on some of these eight regions (regions 4, 5 13 and 14) SMRT binding was reconstituted after 1 to 3 h of ligand application, while for regions 2, 3, 6/7 and 8 the measurement window of 4 h was apparently too short to observe the return of the corepressor. This indicates that for each region an idiosyncratic corepressor association profile exists. A similar individual profile is observed concerning the binding of SRC-1 to the 10 genomic regions. On none of the regions SRC-1 was observed to bind in the absence of ligand and it took 30–240 min of 1α,25(OH)$_2$D$_3$ treatment to observe coactivator association. Moreover, the duration of the SRC-1 association varied between ~1 h for the genomic regions 2, 4, 13 and 14 to >3 h for regions 9 and 10. The association of the mediator TRAP220 and P-Pol II with the 10 genomic regions appeared to be timely coordinated and showed for most regions a peak of ~1 h duration after 1–2 h of ligand treatment. Taken together, the *IGFBP1/3* and *2/5* gene cluster contain 10 VDR- and RXR-associated regions (2, 3, 4, 5, 6/7, 8, 9, 10, 13 and 14), which each shows an individual, ligand-dependent profile of SMRT, SRC-1, TRAP220 and P-Pol II binding.

The *IGFBP2* gene is not transcriptionally regulated by 1α,25(OH)$_2$D$_3$

The REs 9 and 10 are located within the large first intron of the *IGFBP2* gene but are already >17 and 24 kb downstream of the TSS (Figure 2). This raised the question, whether they are involved in the regulation of the *IGFBP2* gene or whether they may regulate the *IGFBP5* gene, although the TSS of the latter gene is even more distant. We tried to answer this question indirectly by assessing via ChIP assays a 1α, 25(OH)$_2$D$_3$-dependent association of VDR with the TSS of the genes *IGFBP1*, *2*, *3* and *5* (Figure 5C). From this it was found that VDR interacts with the proximal promoter of the genes *IGFBP1*, *3* and 5 but not to that of *IGFBP2*. The VDR interaction with the TSS of the *IGFBP1* gene was clearly ligand-dependent with a peak after 1 h stimulation, whereas that on the *IGFBP3* and *5* gene TSS was only weakly modulated by 1α,25(OH)$_2$D$_3$. These findings confirm the real-time quantitative PCR results (Figure 1) that the genes *IGFBP1*, *3* and *5* but not the *IGFBP2* gene are regulated by VDR and its ligand. This observation also suggests that the association of VDR to REs 9 and 10 is not related to a regulation of the gene, *IGFBP2*, in which they are located.

DISCUSSION

This study describes the regulation of multiple *IFGBP* gene family members by the hormone 1α,25(OH)$_2$D$_3$. We confirmed a previous study (10) that *IGFBP3* is a primary VDR target gene and found in addition that its direct genome neighbor, the *IGFBP1* gene, is also a primary target of 1α,25(OH)$_2$D$_3$. Moreover, we even could identify a third family member, the *IGFBP5* gene, as a primary VDR target, whereas the mRNA expression of its tandem partner, the *IGFBP2* gene, was not regulated by the nuclear receptor and its ligand. We observed these primary ligand responses in prostate and bone cancer cells, but it can be assumed that these three genes may also be VDR targets in other 1α,25(OH)$_2$D$_3$ responsive tissues. The 2- to 4-fold induction of *IGFBP1*, *3* and *5* is not a very strong up-regulation, but it is in the order of what was observed with most other 1α, 25(OH)$_2$D$_3$ target genes (29,30). The genes *IGFBP4* and *6* showed in both tested cell lines the highest basal expression of the six *IGFBP* genes, so that a further up-regulation of their expression through 1α,25(OH)$_2$D$_3$ may not be necessary. However, in SaOS-2 cells, which show a significantly lower *IGFBP4* and *6* mRNA expression than PC-3 cells, both genes were shown to be secondary 1α,25(OH)$_2$D$_3$ targets.

Our finding that three members of the *IFGBP* gene family respond to 1α,25(OH)$_2$D$_3$ increases the impact of IGF-1 and the regulation of its circulating amounts by IGFBPs in models of the anti-proliferative action of 1α,25(OH)$_2$D$_3$ and its synthetic analogs (31). In addition, IGFBPs mediate IGF-independent actions, including the activation of the *p21* gene, causing cell cycle arrest or cell death through induction of apoptosis (32). However bound to cellular membranes, IGFBPs can have mitogenic, IGF-dependent effects on cellular growth (33,34). For example, the effect of IGFBP5 induction has been described mitogenic, when induced by androgens in prostate cells (35). This complicates the interpretation of the up-regulation of the IGFBP family members by 1α,25(OH)$_2$D$_3$. The differential regulation of several other primary and secondary 1α,25(OH)$_2$D$_3$ target genes, such as the down-regulation of *IGF-1* and the up-regulation of the *p21* gene, has to be considered in context of the response of IFGBPs. Since the mitogenic effect of IGFBPs is IGF-dependent, 1α,25(OH)$_2$D$_3$ seems to promote the IGF-independent pathway of IGFBPs.

The *in silico* screening performed in this study involved a defined six-member gene family and 174 kb genomic sequence. After a number of carefully selected restrictions the screen resulted in 15 candidate VDREs. ChIP assays indicated that 10 of these 15 REs are bound by VDR in intact PC-3 cells. This represents a 67% success rate of the *in silico* prediction of VDR binding sites, which is much higher than in comparable screenings (36). Moreover, non-ligand responsive genes, such as *IGFBP4* and *6*, did not contain any VDRE candidates, although 24 and 15 kb, respectively, of their genomic sequence were screened. The other non-ligand responsive gene, *IGFBP2*, contains two VDREs (REs 9 and 10) within its first intron. However, ChIP analysis of the proximal promoter region of the *IGFBP2* gene indicated that these VDREs cannot be in contact with the TSS of this gene. It is therefore more probable that they are involved in the regulation of the neighboring *IGFBP5* gene. The high success rate of our combined *in silico* screen/ChIP analysis method suggests that its application on even larger screenings involving megabases of genomic sequence is possible.

It is important to note that our *in silico* screening was not restricted to regulatory regions that comprise only maximal 2 kb of sequence upstream and downstream of the TSS, as in a recent whole genome screen for regulatory elements (37), but involved up to 10 kb upstream sequence, intronic and even intergenic sequences. Therefore, our method reveals candidate

REs that are located at >30 kb distannce from the TSS that is regulated by this VDRE. Based on the present understanding of enhancers, DNA looping and chromatin units being flanked by insulators or matrix attachment sites (38) these distances are no limitations. However, such large distances between RE and TSS cannot be assessed by older experimental approaches, such as transiently transfected promoter reporter gene fusion constructs and the validation of critical promoter regions via truncations or point mutations. In contrast, ChIP assays omit the need of transient transfections and allow the analysis of every region in a genome *in vivo* or *in situ*.

The observation that the *IGFBP1/3* gene cluster contains six functional VDR associated regions (2, 3, 4, 5, 6/7 and 8) and the *IGFBP5* gene area four such regions (9, 10, 13 and 14) supports the model of multiple VDREs per primary 1α, $25(OH)_2D_3$ target gene, which we developed during our analysis of the *CYP24* and *cyclin C* gene (18,19). Interestingly, the VDR-associated genomic regions contain three ER7-type (REs 2, 4 and 5) and one ER9-type (RE 13) VDREs. All four REs showed to bind VDR–RXR heterodimers strongly *in vitro* and are potent VDREs in reporter gene assays. Although synthetic ER7-type VDREs have been known since more than a decade (16), this study demonstrates for the first time the existence of functional ER7-type VDREs *in vivo*. Similarly, the ER9-type RE13 is one of the first natural VDREs of this type. Interestingly, the SNP variation that increases the spacing of this VDRE by 2 nt, forming the ER11-type RE13+, significantly decreases its ability to function as a VDRE *in vitro* and in reporter gene assays. Unfortunately, the SNP variation occurs only with a frequency of 3% in the population, so that we presently have no cellular system testing its effect in ChIP assays.

In conclusion, our study has provided insight into the regulation of the *IGFBP* gene family by $1\alpha,25(OH)_2D_3$. We demonstrated that *IGFBP1*, *3* and *5* are primary 1α, $25(OH)_2D_3$ target genes. Each of these three genes contains multiple functional VDR associated regions in their genomic area suggesting a complex regulation by $1\alpha,25(OH)_2D_3$.

ACKNOWLEDGEMENTS

We would like to thank Dr Lise Binderup for $1\alpha,25(OH)_2D_3$ and Dr Thomas W. Dunlop for critical reading of the manuscript. Grants from the Academy of Finland, the Finnish Cancer Organisation and the Finnish Technology Agency TEKES supported this research. Funding to pay the Open Access publication charges for this article was provided by Academy of Finland.

Conflict of interest statement. None declared.

REFERENCES

1. Sutton,A.L. and MacDonald,P.N. (2003) Vitamin D: more than a 'bone-a-fide' hormone. *Mol. Endocrinol.*, **17**, 777–791.
2. Mørk Hansen,C., Binderup,L., Hamberg,K.J. and Carlberg,C. (2001) Vitamin D and cancer: effects of $1,25(OH)_2D_3$ and its analogs on growth control and tumorigenesis. *Front. Biosci.*, **6**, D820–D848.
3. Jones,G., Strugnell,S.A. and DeLuca,H.F. (1998) Current understanding of the molecular actions of vitamin D. *Physiol. Rev.*, **78**, 1193–1231.
4. Liu,M., Lee,M.-H., Cohen,M., Bommakanti,M. and Freedman,L.P. (1996) Transcriptional activation of the Cdk inhibitor p21 by vitamin D_3 leads to the induced differentiation of the myelomonocytic cell line U937. *Genes Dev.*, **10**, 142–153.
5. Xu,H.M., Tepper,C.G., Jones,J.B., Fernandez,C.E. and Studzinski,G.P. (1993) 1,25-Dihydroxyvitamin D_3 protects HL60 cells against apoptosis but down-regulates the expression of the bcl-2 gene. *Exp. Cell Res.*, **209**, 367–374.
6. Pan,Q. and Simpson,R.U. (1999) c-myc intron element-binding proteins are required for 1,25-dihydroxyvitamin D_3 regulation of c-myc during HL-60 cell differentiation and the involvement of HOXB4. *J. Biol. Chem.*, **274**, 8437–8444.
7. Xie,S.P., Pirianov,G. and Colston,K.W. (1999) Vitamin D analogues suppress IGF-I signalling and promote apoptosis in breast cancer cells. *Eur. J. Cancer*, **35**, 1717–1723.
8. Colston,K.W., Perks,C.M., Xie,S.P. and Holly,J.M. (1998) Growth inhibition of both MCF-7 and Hs578T human breast cancer cell lines by vitamin D analogues is associated with increased expression of insulin-like growth factor binding protein-3. *J. Mol. Endocrinol.*, **20**, 157–162.
9. Huang,Y.C., Chen,J.Y. and Hung,W.C. (2004) Vitamin D_3 receptor/Sp1 complex is required for the induction of p27Kip1 expression by vitamin D_3. *Oncogene*, **23**, 4856–4861.
10. Peng,L., Malloy,P.J. and Feldman,D. (2004) Identification of a functional vitamin D response element in the human insulin-like growth factor binding protein-3 promoter. *Mol. Endocrinol.*, **18**, 1109–1119.
11. Hwa,V., Oh,Y. and Rosenfeld,R.G. (1999) The insulin-like growth factor-binding protein (IGFBP) superfamily. *Endocr. Rev.*, **20**, 761–787.
12. Lee,K.W., Ma,L., Yan,X., Liu,B., Zhang,X.K. and Cohen,P. (2005) Rapid apoptosis induction by IGFBP-3 involves an insulin-like growth factor-independent nucleomitochondrial translocation of RXRalpha/Nur77. *J. Biol. Chem.*, **280**, 16942–16948.
13. Carlberg,C. and Polly,P. (1998) Gene regulation by vitamin D_3. *Crit. Rev. Eukaryot. Gene Expr.*, **8**, 19–42.
14. Quack,M. and Carlberg,C. (2000) Ligand-triggered stabilization of vitamin D receptor/retinoid X receptor heterodimer conformations on DR4-type response elements. *J. Mol. Biol.*, **296**, 743–756.
15. Carlberg,C., Bendik,I., Wyss,A., Meier,E., Sturzenbecker,L.J., Grippo,J.F. and Hunziker,W. (1993) Two nuclear signalling pathways for vitamin D. *Nature*, **361**, 657–660.
16. Schräder,M., Müller,K.M., Nayeri,S., Kahlen,J.P. and Carlberg,C. (1994) VDR-T_3R receptor heterodimer polarity directs ligand sensitivity of transactivation. *Nature*, **370**, 382–386.
17. Schräder,M., Nayeri,S., Kahlen,J.P., Müller,K.M. and Carlberg,C. (1995) Natural vitamin D_3 response elements formed by inverted palindromes: polarity-directed ligand sensitivity of vitamin D_3 receptor–retinoid X receptor heterodimer-mediated transactivation. *Mol. Cell Biol.*, **15**, 1154–1161.
18. Väisänen,S., Dunlop,T.W., Sinkkonen,L., Frank,C. and Carlberg,C. (2005) Spatio-temporal activation of chromatin on the human CYP24 gene promoter in the presence of 1alpha,25-dihydroxyvitamin D_3. *J. Mol. Biol.*, **350**, 65–77.
19. Sinkkonen,L., Malinen,M., Saavalainen,K., Väisänen,S. and Carlberg,C. (2005) Regulation of the human cyclin C gene via multiple vitamin D_3 -responsive regions in its promoter. *Nucleic Acid Res.*, **33**, 2440–2451.
20. Burke,L.J. and Baniahmad,A. (2000) Co-repressors 2000. *FASEB J.*, **14**, 1876–1888.
21. Polly,P., Herdick,M., Moehren,U., Baniahmad,A., Heinzel,T. and Carlberg,C. (2000) VDR-Alien: a novel, DNA-selective vitamin D_3 receptor–corepressor partnership. *FASEB J.*, **14**, 1455–1463.
22. Leo,C. and Chen,J.D. (2000) The SRC family of nuclear receptor coactivators. *Gene*, **245**, 1–11.
23. Castillo,A.I., Jimenez-Lara,A.M., Tolon,R.M. and Aranda,A. (1999) Synergistic activation of the prolactin promoter by vitamin D receptor and GHF-1: role of coactivators, CREB-binding protein and steroid hormone receptor coactivator-1 (SRC-1). *Mol. Endocrinol.*, **13**, 1141–1154.
24. Fondell,J.D., Guermah,M., Malik,S. and Roeder,R.G. (1999) Thyroid hormone receptor-associated proteins and general positive cofactors mediate thyroid hormone receptor function in the absence of the TATA box-binding protein-associated factors of TFIID. *Proc. Natl Acad. Sci. USA*, **96**, 1959–1964.
25. Rachez,C., Lemon,B.D., Suldan,Z., Bromleigh,V., Gamble,M., Näär,A.M., Erdjument-Bromage,H., Tempst,P. and Freedman,L.P. (1999) Ligand-dependent transcription activation by nuclear receptors requires the DRIP complex. *Nature*, **398**, 824–828.

26. Levin,A.A., Sturzenbecker,L.J., Kazmer,S., Bosakowski,T., Huselton,C., Allenby,G., Speck,J., Kratzeisen,C., Rosenberger,M., Lovey,A. *et al.* (1992) 9-*Cis* retinoic acid stereoisomer binds and activates the nuclear receptor RXRα. *Nature*, **355**, 359–361.
27. Kahlen,J.P. and Carlberg,C. (1996) Functional characterization of a 1,25-dihydroxyvitamin D_3 receptor binding site found in the rat atrial natriuretic factor promoter. *Biochem. Biophys. Res. Commun.*, **218**, 882–886.
28. Toell,A., Polly,P. and Carlberg,C. (2000) All natural DR3-type vitamin D response elements show a similar functionality in vitro. *Biochem. J.*, **352**, 301–309.
29. Swami,S., Raghavachari,N., Muller,U.R., Bao,Y.P. and Feldman,D. (2003) Vitamin D growth inhibition of breast cancer cells: gene expression patterns assessed by cDNA microarray. *Breast Cancer Res. Treat.*, **80**, 49–62.
30. Palmer,H.G., Sanchez-Carbayo,M., Ordonez-Moran,P., Larriba,M.J., Cordon-Cardo,C. and Munoz,A. (2003) Genetic signatures of differentiation induced by 1α,25-dihydroxyvitamin D_3 in human colon cancer cells. *Cancer Res.*, **63**, 7799–7806.
31. Rozen,F. and Pollak,M. (1999) Inhibition of insulin-like growth factor I receptor signaling by the vitamin D analogue EB1089 in MCF-7 breast cancer cells: A role for insulin-like growth factor binding proteins. *Int. J. Oncol.*, **15**, 589–594.
32. Krishnan,A.V., Peehl,D.M. and Feldman,D. (2003) The role of vitamin D in prostate cancer. *Recent Results Cancer Res.*, **164**, 205–221.
33. Kelley,K.M., Oh,Y., Gargosky,S.E., Gucev,Z., Matsumoto,T., Hwa,V., Ng,L., Simpson,D.M. and Rosenfeld,R.G. (1996) Insulin-like growth factor-binding proteins (IGFBPs) and their regulatory dynamics. *Int. J. Biochem. Cell Biol.*, **28**, 619–637.
34. Yin,P., Xu,Q. and Duan,C. (2004) Paradoxical actions of endogenous and exogenous insulin-like growth factor-binding protein-5 revealed by RNA interference analysis. *J. Biol. Chem.*, **279**, 32660–32666.
35. Gregory,C.W., Kim,D., Ye,P., D'Ercole,A.J., Pretlow,T.G., Mohler,J.L. and French,F.S. (1999) Androgen receptor up-regulates insulin-like growth factor binding protein-5 (IGFBP-5) expression in a human prostate cancer xenograft. *Endocrinology*, **140**, 2372–2381.
36. Wasserman,W.W. and Sandelin,A. (2004) Applied bioinformatics for the identification of regulatory elements. *Nature Rev. Genet.*, **5**, 276–287.
37. Xie,X., Lu,J., Kulbokas,E.J., Golub,T.R., Mootha,V., Lindblad-Toh,K., Lander,E.S. and Kellis,M. (2005) Systematic discovery of regulatory motifs in human promoters and 3′ UTRs by comparison of several mammals. *Nature*, **434**, 338–345.
38. Ogata,K., Sato,K. and Tahirov,T.H. (2003) Eukaryotic transcriptional regulatory complexes: cooperativity from near and afar. *Curr. Opin. Struct. Biol.*, **13**, 40–48.